

Supporting Information for

Development and evaluation of E3SM-MOSAIC: Spatial distributions and radiative effects of nitrate aerosol

Mingxuan Wu¹, Hailong Wang¹, Richard C. Easter¹, Zheng Lu², Xiaohong Liu²,
Iwinder Singh¹, Po-Lun Ma¹, Qi Tang³, Rahul Zaveri¹, Ziming Ke², Rudong Zhang¹,
Louisa K. Emmons⁴, Simone Tilmes⁴, Jack E. Dibb⁵, Xue Zheng³, Shaocheng Xie³, L.

Ruby Leung¹

¹Atmospheric Sciences and Global Change Division, Pacific Northwest National Laboratory, Richland, WA, USA

²Department of Atmospheric Sciences, Texas A&M University, College Station, TX, USA

³Lawrence Livermore National Laboratory, Livermore, CA, USA

⁴National Center for Atmospheric Research, Boulder, CO, USA

⁵Earth Systems Research Center, Institute for the Study of Earth, Oceans, and Space, University of New Hampshire,

Durham, NH, USA

15

16

17

18

10

20

22

23 **Contents of this file**

24 Figures S1 to S13

25 Tables S1 to S4

26

27 **Introduction**

28 In the Supporting Information section, we prepared 13 figures and 4 tables to support the
29 main manuscript. Table S1 gives the mass budget of nitrate in MTC_SPLAC and
30 MTC_FAST. Table S2 gives the mass budget of sulfate from 5 E3SM experiments. Table

31 S3 lists the tropospheric HNO₃ burden in the three MOSAIC experiments compared with
32 other studies. Table S4 lists the mean surface molar concentrations of aerosols and gases
33 for Figures 4 and 5 in the main manuscript. Figure S1 evaluates the modeled tropospheric
34 column ozone against OMI/MLS retrievals. Figure S2 compares modeled tropospheric
35 C₂H₆, C₃H₈, C₂H₂, and C₂H₄ with summaries of observations from aircraft campaigns.

36 Figure S3 shows the spatial distributions of nitrate column mass tendencies due to
37 aqueous chemistry and gas-aerosol exchange. Figure S4 shows the spatial distributions of
38 ammonium burden. Figure S5 shows the latitude-altitude cross sections of nitrate
39 concentrations. Figure S6 evaluates modeled surface concentrations of nitrate aerosols
40 and HNO₃ from Zaveri et al. (2021) and Lu et al. (2021) against observations at
41 CASTNET, EMEP, and EANET network sites. Figure S7 evaluates modeled surface
42 concentrations of NO_x against observations at AQS, EMEP, and EANET network sites.

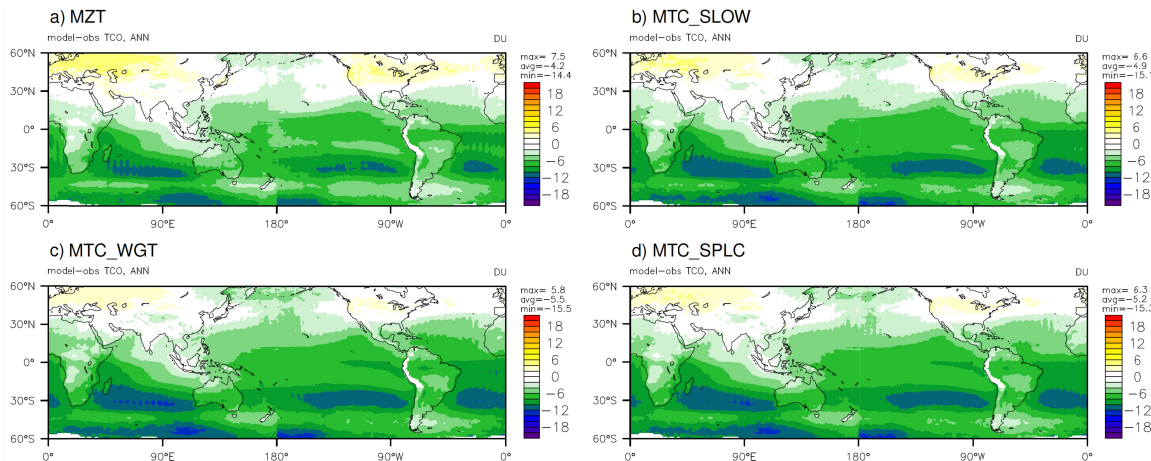
48 Figures S8-S10 show the seasonal variations of simulated and observed sulfate, HNO₃,
 49 and ammonium surface concentrations at 6 CASTNET sites. Figures S11 and S12
 50 compare vertical profiles of HNO₃ concentrations from model simulations with
 51 observations from INTEX-B, ARCTAS, DC3, SEAC⁴RS, and ATom campaigns. Figure
 52 S13 shows the spatial distributions of RFari of ammonium aerosols.

49

50

51

52



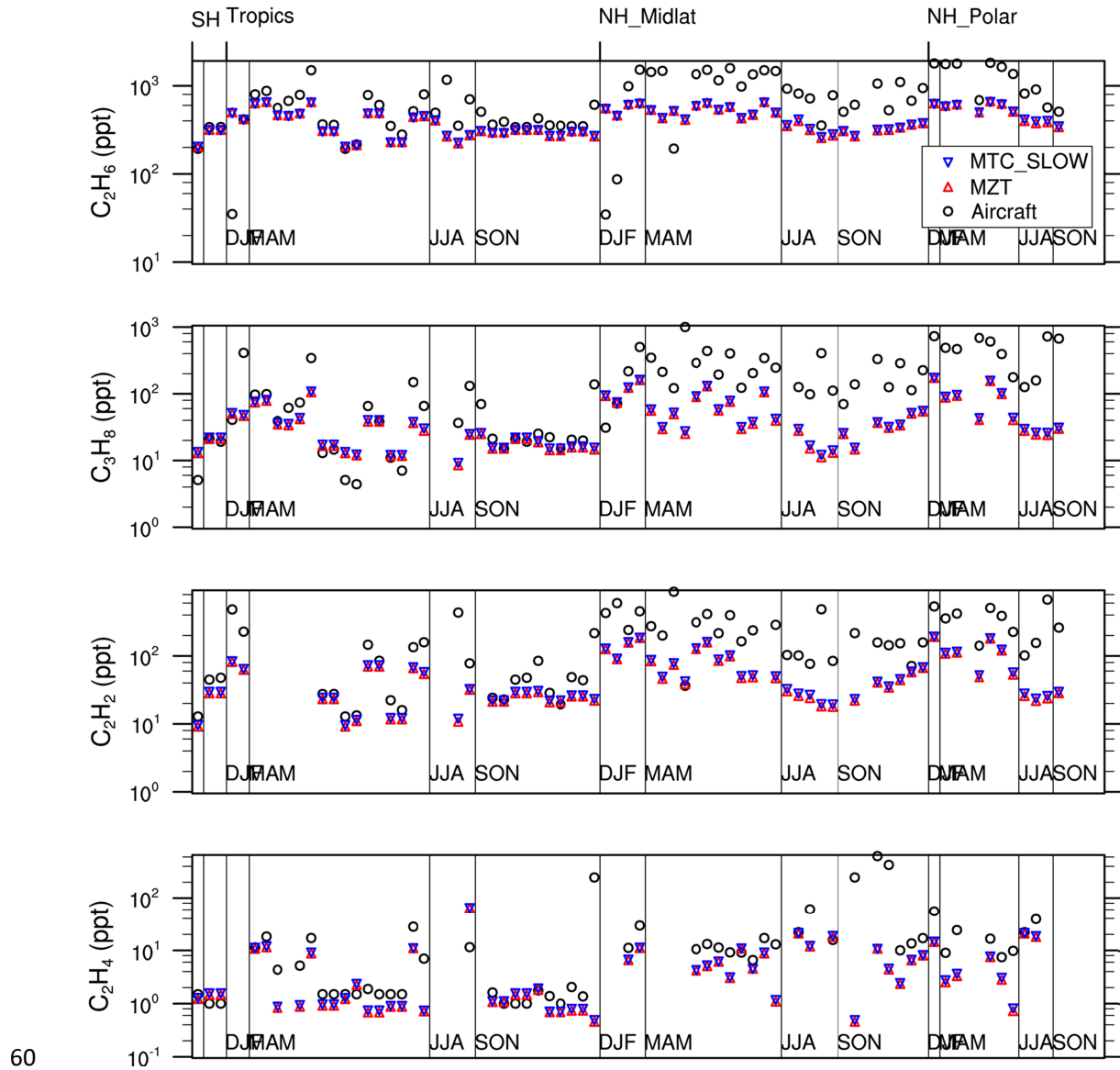
53 **Figure S1.** Spatial distributions of global annual mean tropospheric column ozone
 55 differences compared with OMI/MLS retrievals.
 56

56

57

58

59



63 **Figure S2.** Evaluation of modeled tropospheric C_2H_6 , C_3H_8 , C_2H_2 , and C_2H_4 (averaged
 64 over 2005-2014) with summaries of observations from aircraft campaigns (operated
 65 during 1995-2010), averaged over 2-7 km.

64

65

66

67

68

71 **Figure S3.** Spatial distributions of nitrate column mass tendencies ($\mu\text{g m}^{-2} \text{s}^{-1}$) due to
 72 (a-c) aqueous chemistry (AQCH), (d-f) gas-aerosol exchange (GAEX), (g-i) gas-aerosol
 73 exchange in the fine mode, and (j-l) gas-aerosol exchange in the coarse mode.

72

73

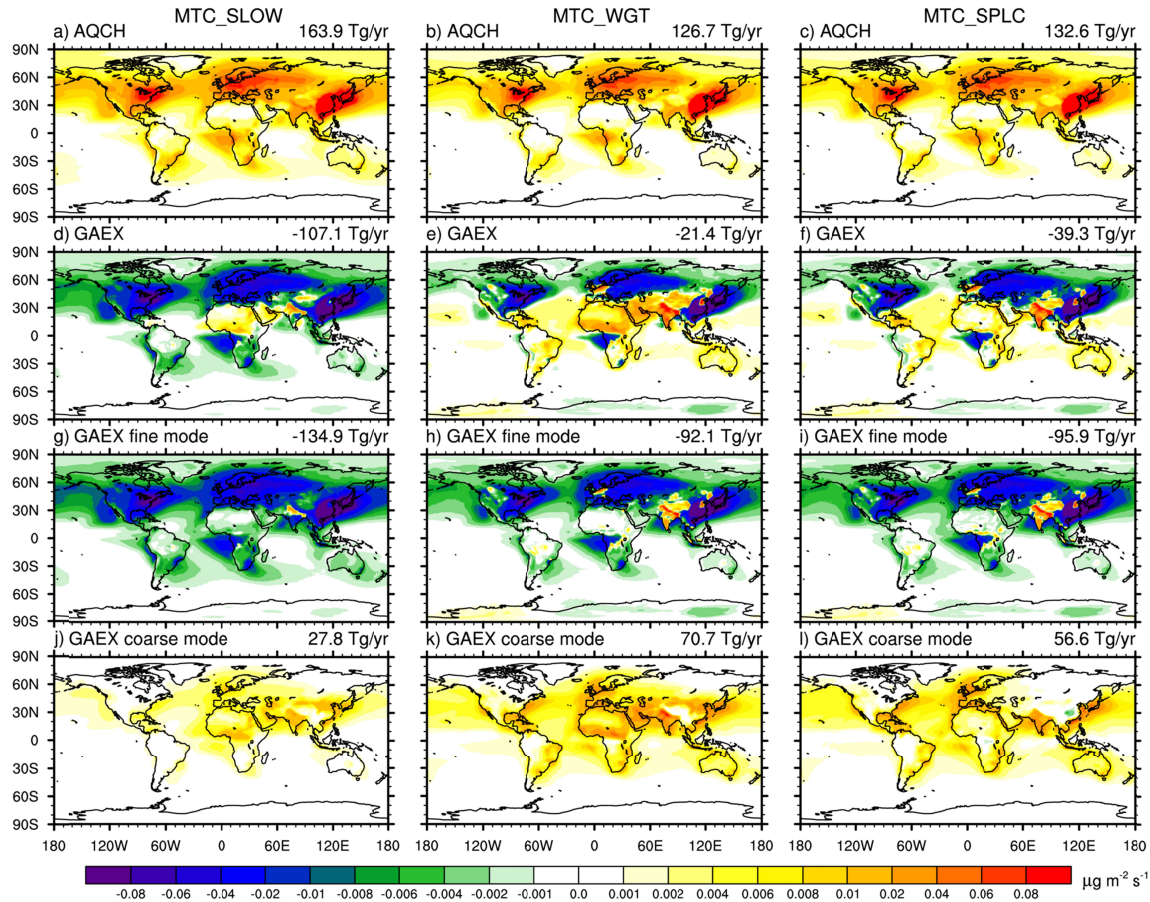
74

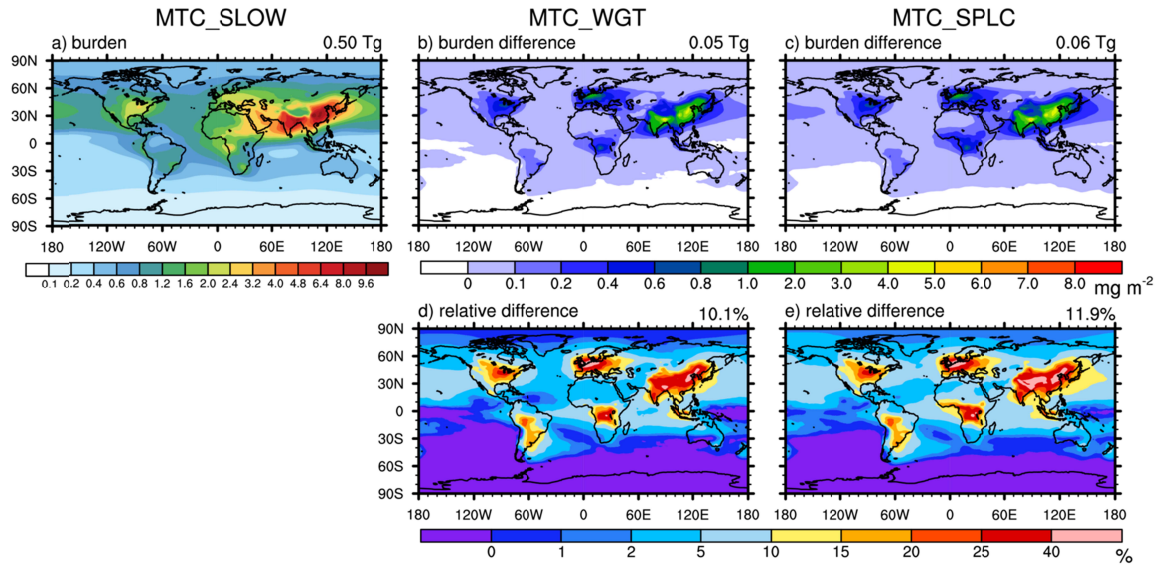
75

76

77

78





79

83 **Figure S4.** Spatial distributions of global annual mean (a) ammonium burden
 84 (MTC_SLOW), (b-c) ammonium burden differences (MTC_WGT and MTC_SPLC)
 85 compared to MTC_SLOW, and (d-e) relative differences of ammonium burden compared
 86 to MTC_SLOW. Numbers at the top-right of each panel are global annual mean values.

84

85

86

87

88

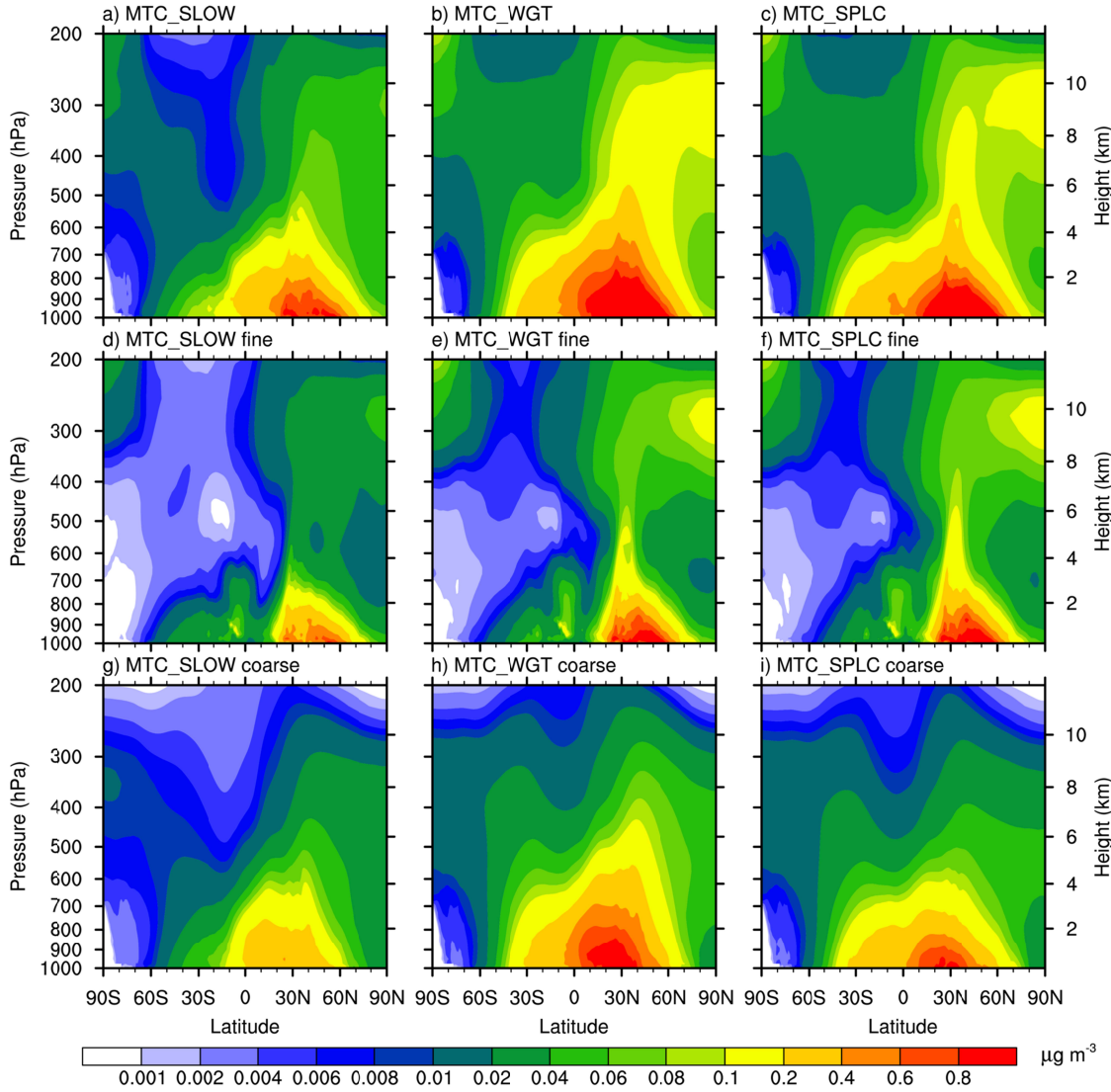
89

90

91

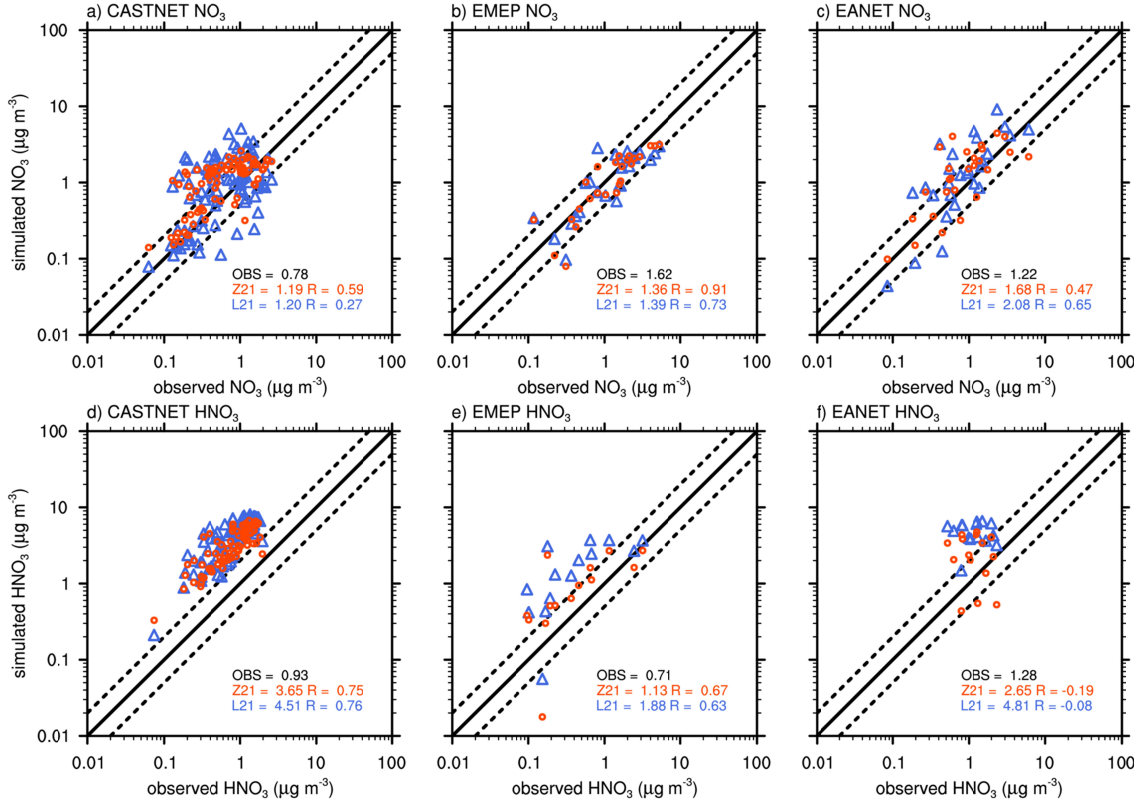
92

93



94

96 **Figure S5.** Latitude-altitude cross sections of annually averaged zonal mean (a-c) total,
 97 (d-f) fine mode, and (g-i) coarse mode nitrate concentrations ($\mu\text{g m}^{-3}$).
 98
 99
 100
 101



102

107 **Figure S6.** Scatter plots of modeled annual mean surface concentrations ($\mu\text{g m}^{-3}$) of
 108 nitrate aerosols (top row) and HNO₃ (bottom row) from Zaveri et al. (2021) (2000-2005)
 109 and Lu et al. (2021) (2005-2007) compared to observations at CASTNET (left column),
 110 EMEP (middle column), and EANET (right column) network sites during 2005-2014.

111 The numbers are mean concentrations and correlation coefficients.

108

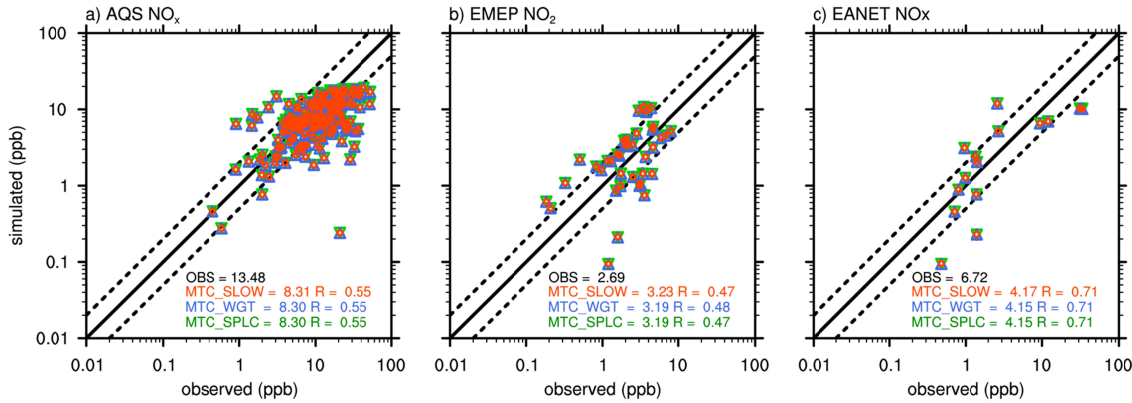
109

110

111

112

113



114

119 **Figure S7.** Scatter plots of modeled annual mean surface concentrations of NO_x (ppb)
 120 compared to observations at AQS and EANET network sites and NO₂ (ppb in STP;
 121 converted from $\mu\text{g m}^{-3}$) compared to observations at EMEP network sites. We only select
 122 rural and suburban sites for AQS network. The numbers are mean concentrations and
 123 correlation coefficients.

120

121

122

123

124

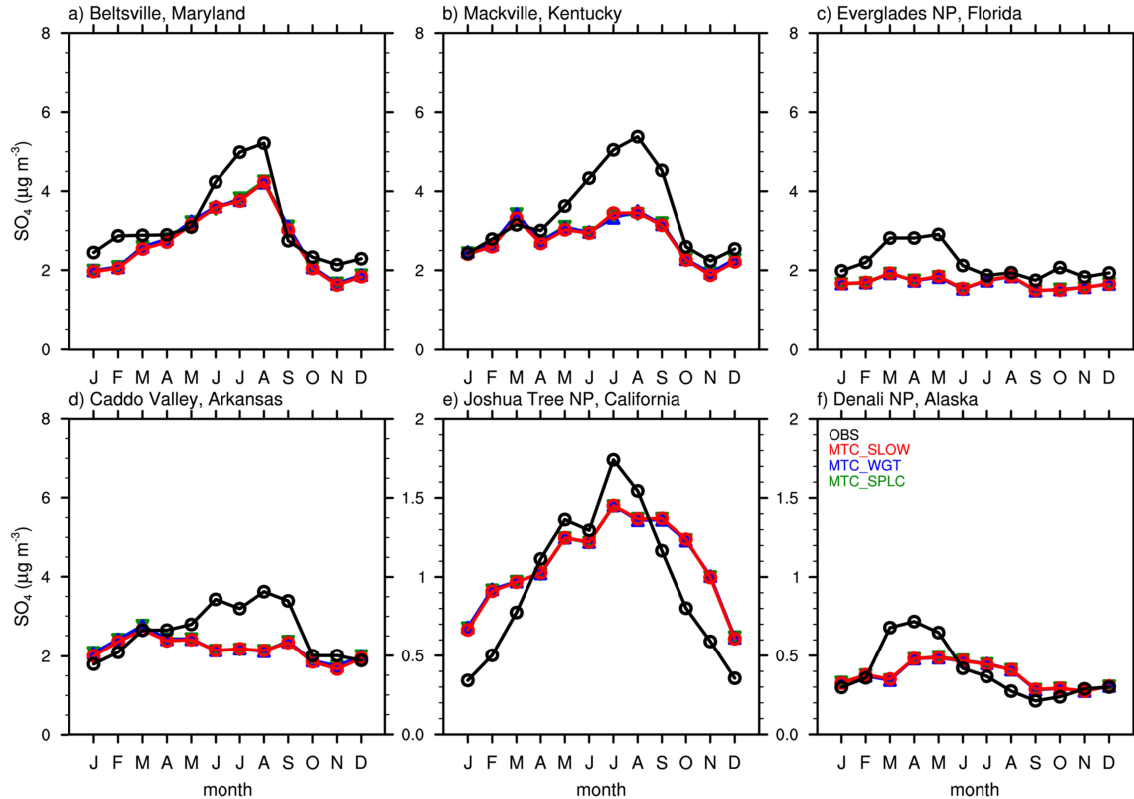
125

126

127

128

129



130

132 **Figure S8.** Seasonal variations of simulated (color lines and symbols) and observed
 133 (black lines and circles) sulfate surface concentrations ($\mu\text{g m}^{-3}$) at six CASTNET sites.
 134

135

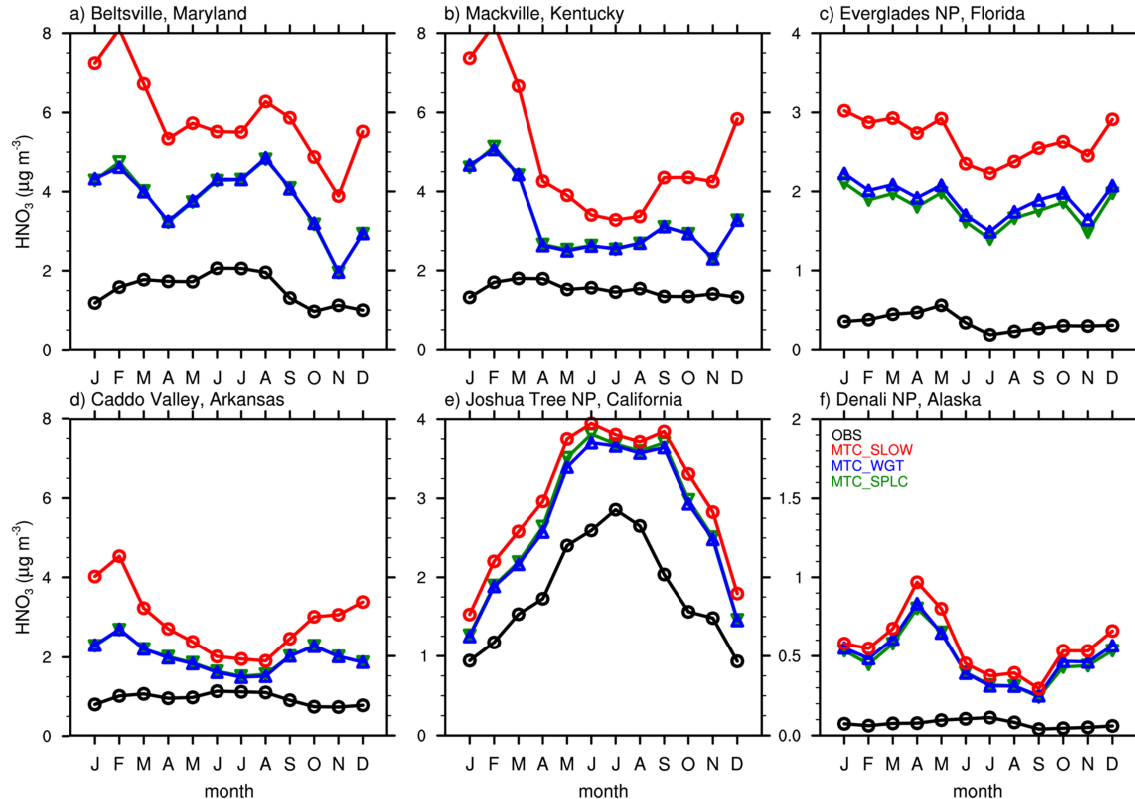
136

137

138

139

140



141

143 **Figure S9.** Seasonal variations of simulated (color lines and symbols) and observed
 144 (black lines and circles) HNO_3 surface concentrations ($\mu\text{g m}^{-3}$) at six CASTNET sites.

144

145

146

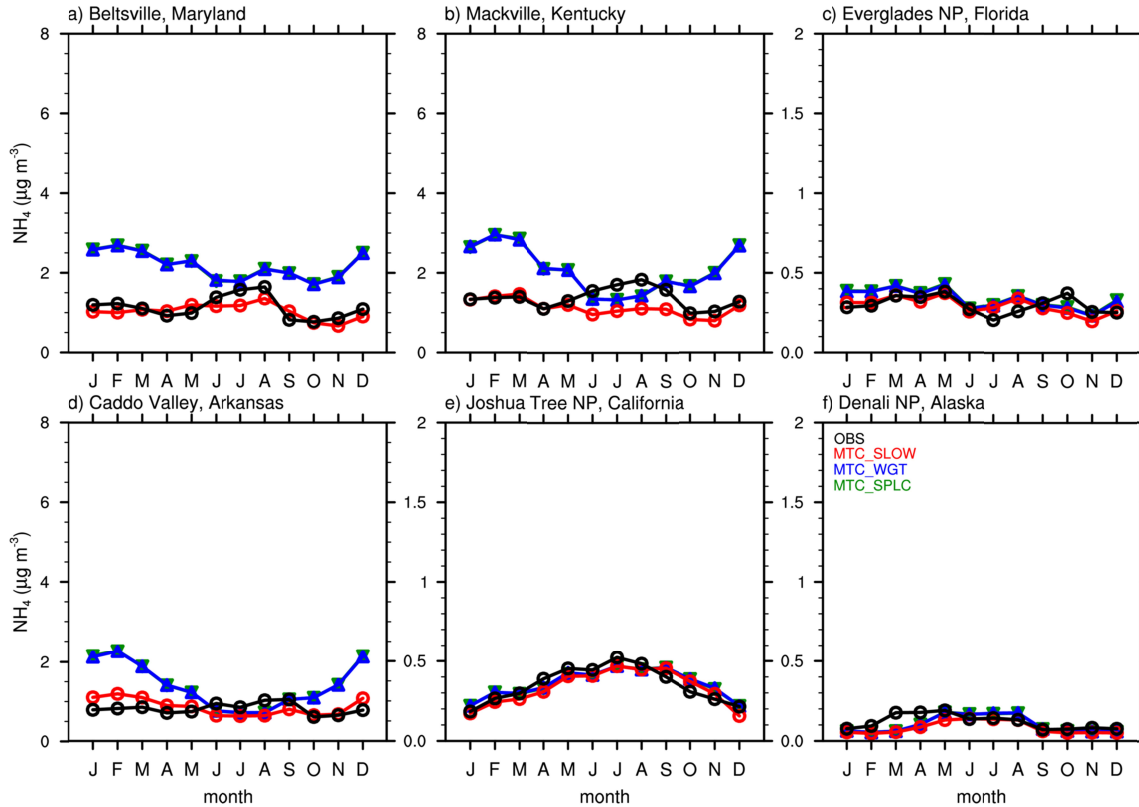
147

148

149

150

151



152

155 **Figure S10.** Seasonal variations of simulated (color lines and symbols) and observed
 156 (black lines and circles) ammonium surface concentrations ($\mu\text{g m}^{-3}$) at six CASTNET
 157 sites.

156

157

158

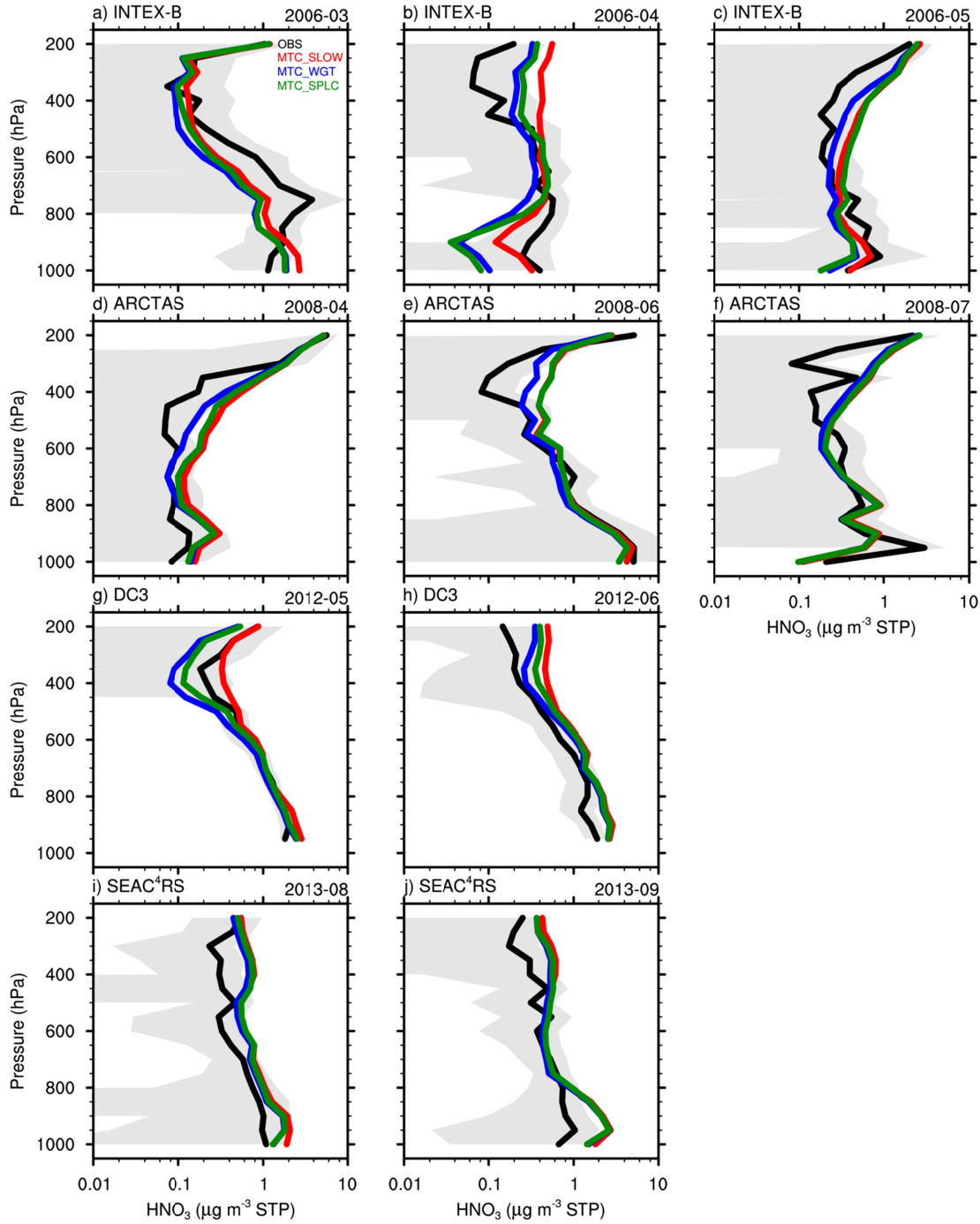
159

160

161

162

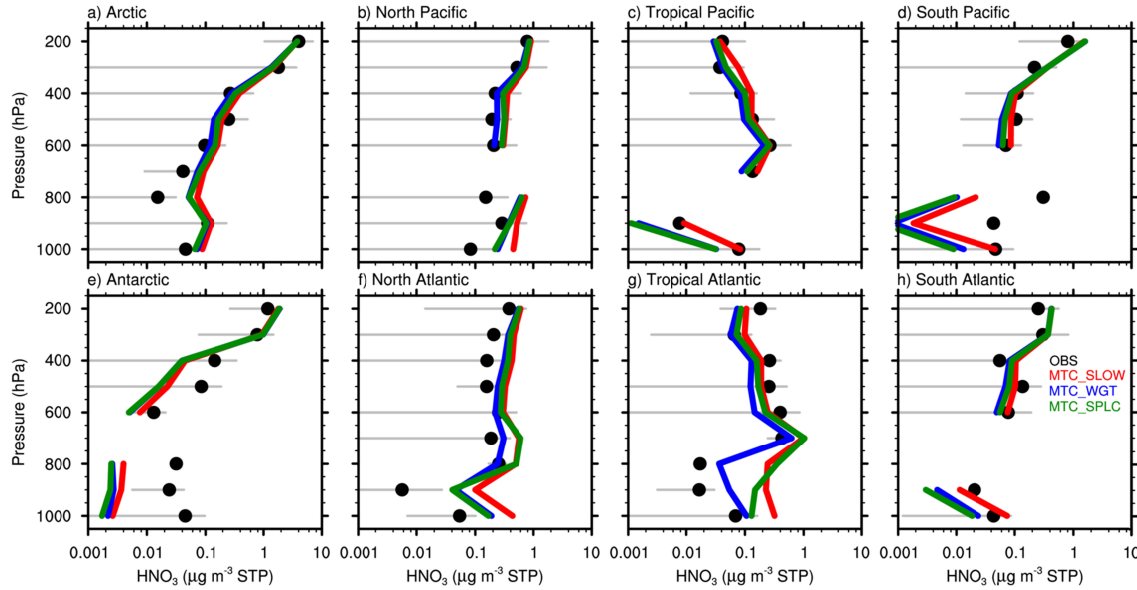
163



164

167 **Figure S11.** Vertical profiles of HNO₃ concentrations ($\mu\text{g m}^{-3}$ in STP) from model
 168 simulations (colored lines) and four aircraft campaigns (dark solid lines for mean values;
 169 shaded areas for plus/minus one standard deviation of observations).

168



169

172 **Figure S12.** Vertical profiles of HNO₃ concentrations ($\mu\text{g m}^{-3}$ in STP) from model
173 simulations (colored lines) and ATom campaign (black dots for mean values; grey lines
174 for plus/minus one standard deviation of observations).

173

174

175

176

177

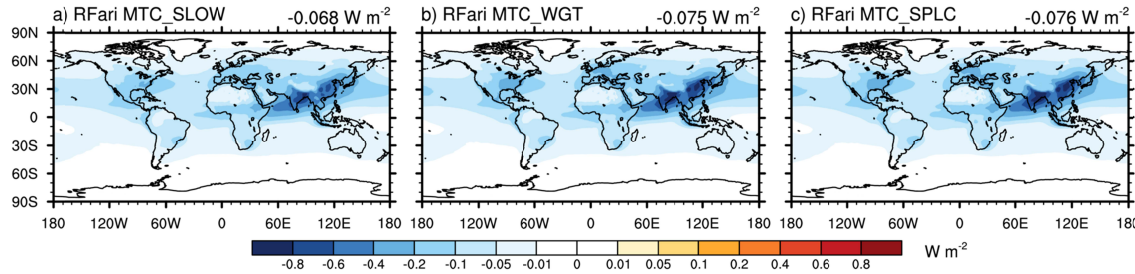
178

179

180

181

182



183

185 **Figure S13.** Spatial distributions of RFari of ammonium aerosols between 1850 and
186 2010.

186

187

188

189

190

191

192

193

194

195

196

197

198

199

200

200 **Table S1.** Mass Budgets of Nitrate in MTC_SPLAC and MTC_FAST

NO_3	MTC_FAST	MTC_SPLAC
Aqueous Chemistry (Tg N a^{-1})	26.8 (26.8, 0.1)	29.4 (29.3, 0.1)
Gas-aerosol Exchange (Tg N a^{-1})	-0.4 (-19.7, 19.2)	-7.9 (-21.0, 13.1)
Net Chemistry Production (Tg N a^{-1})	26.4 (7.1, 19.3)	21.1 (8.3, 13.2)
Dry Deposition (Tg N a^{-1})	11.3 (1.5, 9.8)	8.4 (1.7, 6.7)
Wet Deposition (Tg N a^{-1})	15.0 (5.6, 9.5)	13.1 (6.6, 6.5)
Burden (Tg N)	0.256 (0.061, 0.194)	0.191 (0.080, 0.111)
Lifetime (day)	3.54 (3.18, 3.68)	3.25 (3.51, 3.08)

201 Note. Values in parentheses are for the fine (accumulation and Aitken mode) and coarse
202 modes, respectively.

203

204 **Table S2.** Mass Budgets of nss-Sulfate

nss- SO_4	Default	MZT	MTC_SLOW	MTC_WGT	MTC_SPLC
Emission (Tg S a^{-1})	1.81	1.81	1.81 (61.89)	1.81 (61.92)	1.81 (61.89)
Aqueous chemistry (Tg S a^{-1})	24.18	19.29	20.08	20.09	19.41
Gas-aerosol exchange (Tg S a^{-1})	15.80	12.93	12.65	12.51	12.60
Dry deposition (Tg S a^{-1})	8.79	8.11	8.37 (52.88)	8.24 (52.82)	8.24 (52.80)
Wet deposition (Tg S a^{-1})	33.12	26.36	26.99 (42.58)	26.96 (42.53)	27.01 (42.57)
Burden (Tg S)	0.784	0.703	0.706 (0.844)	0.702 (0.840)	0.705 (0.843)
Life time (day)	6.83	7.45	7.29 (3.23)	7.27 (3.22)	7.29 (3.23)

205 Note. Values in parentheses are for total sulfate, including ss-sulfate.

206

207

208

209

210

211

212

213 **Table S3.** Tropospheric HNO₃ burden in the Three E3SM Experiments Compared with

214 Other Studies

	Burden (Tg N) ^a
MTC_SLOW	0.425
MTC_WGT	0.353
MTC_SPLC	0.389
Bian et al. (2017)	0.56 [0.15, 1.3] ^b 0.39 [0.15, 0.69] ^c
Lu et al. (2021)	0.637
Zaveri et al. (2021)	0.422
Xu & Penner (2012)	0.30
Feng & Penner (2007)	0.37

215 ^aValues are calculated as pressure > 100 hPa for Bian et al. (2017), Lu et al. (2021),
 216 Zaveri et al. (2021), and this study; pressure > 150 hPa for Xu and Penner (2012); and
 217 pressure > 200 hPa for Feng and Penner (2007). ^bValues in brackets are minimum and
 218 maximum values, respectively. ^cWe select 4 GCMs which simulate the formation of
 219 nitrate aerosols in both the fine and coarse modes and consider the heterogeneous
 220 reactions on dust and sea salt particles.

221

222

223

224

225

226

227

228

229

230

231

232 **Table S4.** Mean Surface Molar Concentrations (ppb in STP; converted from $\mu\text{g m}^{-3}$) of

233 Aerosols and Precursor Gases for Figures 4 and 5.

Region	Specie	Observation	MTC_SLOW	MTC_WGT	MTC_SPLC
U.S.	NO_3	0.28	0.43	1.01	1.01
	HNO_3	0.33	1.30	0.97	0.97
	NO_3+HNO_3	0.61	1.72	1.98	1.98
	NH_4	0.97	0.92	1.54	1.54
	NH_3	2.17	1.90	1.47	1.47
	NH_4+NH_3	3.14	2.82	3.01	3.02
	SO_4	0.49	0.46	0.46	0.46
	SO_2	0.72	1.32	1.33	1.33
Europe	NO_3	0.56	0.53	1.18	1.17
	HNO_3	0.25	0.70	0.44	0.44
	NO_3+HNO_3	0.82	1.23	1.62	1.61
	NH_4	1.06	0.77	1.60	1.60
	NH_3	1.70	2.45	1.87	1.87
	NH_4+NH_3	2.76	3.22	3.47	3.47
	SO_4	0.42	0.34	0.35	0.35
	SO_2	0.47	1.00	1.00	1.00
East Asia	NO_3	0.44	0.53	1.21	1.19
	HNO_3	0.45	1.92	1.37	1.38
	NO_3+HNO_3	0.89	2.44	2.58	2.57
	NH_4	1.28	1.43	2.16	2.19
	NH_3	2.48	2.13	1.69	1.69
	NH_4+NH_3	3.76	3.56	3.84	3.87
	SO_4	0.87	0.83	0.84	0.84
	SO_2	2.46	2.37	2.38	2.39

234

235

236

237